First crystal-structure determination of chromites from an acapulcoite and ordinary chondrites

Davide Lenaz[1*], Francesco Princivalle[1] and Birger Schmitz[2,3]

[1]Department of Mathematics and Geosciences, University of Trieste, Trieste, Italy

[2]Division of Nuclear Physics, Department of Physics, Lund University, Lund, Sweden

[3]Hawai'i Institute of Geophysics and Planetology, University of Hawai'i at Manoa,
Honolulu, HI, USA

Submitted to:
Mineralogical Magazine

* Corresponding Author
e-mail address: lenaz@units.it (D. Lenaz)

ABSTRACT – We report the first crystal structure determinations of chromites from an acapulcoite and from ordinary chondrites. Cell edges range from 8.3212 (3) to 8.3501 (1) Å, while the oxygen positional parameters are in the range 0.2624 (3) to 0.26298 (9). Their compositions show they are very close to the chromite end-member $FeCr_2O_4$ with limited Al and Mg content. Titanium oxide content exceeds 1%, whereas the amount of Fe^{3+} is negligible. Extraterrestrial chromite is readily distinguished from terrestrial analogues on the basis of cell edge and oxygen positional parameter. These distinctions will facilitate ongoing attempts to reconstruct the paleoflux of meteorites to Earth from resistant extraterrestrial spinel grains recovered from ancient sediments.

Keywords: chromite; acapulcoite; ordinary chondrite; X-ray single crystal diffraction; meteorite flux

1. INTRODUCTION

Chromite is a minor but regular constituent of ordinary chondrites and its chemistry in meteorites has been studied since the 1960's. Bunch *et al.* (1967) were the first to give a survey of the chemical composition of chondritic chromites. They suggested that there is a relationship between chromite Fe-Mg contents and olivine Fe-Mg contents in the H, L and LL groups of equilibrated chondrites. Besides the main components FeO and Cr_2O_3, chromite contains minor amounts of MgO and Al_2O_3. The increase in $Fe^{2+}/(Fe^{2+}+Mg)$ from H to LL chondrites is evident. Nonetheless, Wlotzka (2005) argued it was not possible to distinguish between the H and L groups from the chromite composition alone, as has been attempted for fossil chondrites (Bridges *et al.,* 2007), because of the overlapping $Fe^{2+}/(Fe^{2+}+Mg)$ ratios of chromites. Besides Al and Mg, Ti is a major element in the chromite. Although there is overlap in the composition of chromites from H, L and LL chondrites, the average element composition of a larger set of chromite grains from fossil meteorite gives an indication of the dominant origin of the grains (Schmitz, 2013). This relation has been confirmed by oxygen isotopic analyses of chromites from fossil Ordovician meteorites showing that these indeed are dominantly pseudomorphosed L chondrites, as indicated by their chromite chemical composition (Heck *et al*., 2010). Acapulcoites are coarsely crystalline, unshocked objects of chondritic composition and igneous texture (Palme *et al*., 1981; Folco *et al*., 2006; Rubin, 2007). Equilibration temperatures for acapulcoites are much higher than those estimated for the most equilibrated ordinary chondrites (950-1250 K; Dodd, 1969). Oxygen-three isotopes indicate possible aqueous alteration of acapulcoites prior to the onset of thermal metamorphism (Greenwood *et al*., 2012), and a comparison of chromite from acapulcoites and ordinary chondrites is thus of interest.

It is well known that terrestrial Cr-bearing spinel can be considered as a petrogenetic indicator because chromite composition is a rich source of information on the origin and evolution of its parent magmas (Irvine, 1967; Dick and Bullen, 1984). The relationships between composition, structural parameters and genetic environment of Cr-bearing spinels from different terrestrial occurrences have been considered by several authors for a better understanding of their genesis and/or oxidation mechanisms (Della Giusta *et al*., 1986; Princivalle *et al*., 1989; Carbonin *et al*., 1999; Carraro, 2003; Bosi *et al*., 2004; Uchida *et al*., 2005; Lenaz *et al*., 2010, 2011; Derbyshire *et al*., 2013; Princivalle *et al*., 2014).

This study presents the first structural and chemical data of meteoritic chromite. Data are given for a total of nine chromite grains, including one from an acapulcoite (labeled ACAP), and four each from the Kernouvé H6 ordinary chondrite (H6) and from an ~ 470 Ma old fossil meteorite, Gol 001 (GOL), found in Ordovician limestone at Kinnekulle in Sweden and originating from the coeval disruption of the L-chondrite parent body (Schmitz et al., 2001; Heck *et al.*, 2010; Schmitz, 2013). Recently, Alwmark and Schmitz (2009) and Heck et al. (2010) distinguished terrestrial and extraterrestrial chromite using relict silicate inclusions and high-precision oxygen three-isotopes SIMS analyses, respectively. As these analyses are time-consuming and necessitate a lot of material, our study aims to determine whether structural parameters, such as cell edge and oxygen positional parameter, can be used to distinguish extraterrestrial from terrestrial chromite. Since structure refinement requires much less material, this will facilitate ongoing attempts to reconstruct the paleoflux of meteorites to Earth from resistant extraterrestrial spinel grains recovered from ancient sediments.

2. MATERIALS AND BACKGROUND

Acapulcoites belong to the class of acapulcoite-lodranite (A-L) meteorites (McCoy *et al.*, 1993). A high degree of recrystallization and mineral chemical data indicate formation of acapulcoites under redox conditions intermediate between those of H- and E-chondrites, at about 1100°C, from which it cooled at a rate > l0°C/Ma (Dodd, 1969). The major element composition is within the range of H-chondrites. Troilite and metal are heterogeneously distributed. Associated trace elements are heterogeneously distributed whereas chromium content is a factor of two higher than in H-chondrites. Acapulcoites consist of an assemblage of orthopyroxene, olivine and feldspar associated with comparatively large amounts of metallic nickel-iron, and minor amounts of diopside, troilite, chromite and phosphate. The chromite is rather constant in composition from grain to grain and appears to be distinct from chromite in ordinary chondrites (Bunch *et al.*, 1967), silicate inclusions of iron meteorites (Bunch *et al.*, 1970), pallasites, mesosiderites, and eucrites (Bunch and Keil, 1971). The distribution of divalent cations fits into the correlation observed for equilibrated meteorites. The high concentrations of Cr, Mn and Zn in chromites are also observed in chromite from silicate inclusions of iron meteorites. ZnO concentrations in acapulcoite chromites range from 0.9 to 1.3%; these relatively high contents reflect the unusually high bulk Zn content of acapulcoite (Palme *et al*., 1981).

Kernouvé is an ordinary chondrite of the H group from an observed fall in France in 1869. It is texturally metamorphosed and of petrologic type 6. It contains abundant metals, was heated for a significant period of time before the onset of partial melting, and is minimally shocked (Ford *et al*., 2008). It contains relict chondrules set in a coarse-grained, recrystallized matrix of olivine (Fo_{80}), orthopyroxene ($Fs_{15.7\text{-}18.1}$), plagioclase, Fe-Ni metal, troilite, chromite and phosphate (Ford *et al*., 2008). Chromite grains from this chondrite are chemically homogeneous and have the typical equilibrated H-chondritic composition with generally somewhat lower TiO_2 (~2.5 wt%) and higher Al_2O_3 (~6.0 wt%) contents than equilibrated L chondrites (typically TiO_2 ~3.0 wt% and Al_2O_3 ~ 5.2 wt%) (Bunch *et al*., 1967; Schmitz *et al*., 2001).

Meteorite Gol 001 (formal name Österplana 029) is a relatively large (6 x 9 x 2 cm) mid-Ordovician fossil meteorite found in the Golvsten bed in the Thorsberg quarry in southern Sweden (Schmitz *et al*., 2001). The meteorite contains abundant, large and well-preserved chromite grains. Chromite grains are homogeneous in chemical composition throughout the meteorite, and the average composition of several of the grains plots with equilibrated L chondrites (Schmitz *et al*., 2001). Based on these data and the maximum chromite grain diameter, Bridges *et al*. (2007) assigned it to the L6 group and type. Oxygen-three isotopic analyses of the chromite grains confirm an L or LL chondritic origin (Greenwood *et al*., 2007; Heck *et al*., 2010). The cosmic-ray exposure age of meteorite Gol 001 is ca. 300 kyr based on noble (neon) gas isotopic measurements of chromite grains from the meteorite (Heck *et al*., 2004). This age concurs very well with the estimated timing of the break-up of the L chondrite parent-body based on the stratigraphic first appearance of abundant sediment-dispersed chromite grains from L-chondritic micrometeorites (Schmitz, 2013). Altogether the isotopic and chemical data show that the chromite grains from this meteorite are excellently preserved despite having been buried in marine limestone for 470 Ma.

3. METHODS

X-ray diffraction data for the nine chromite grains analyzed were recorded on an automated KUMA-KM4 (K-geometry) diffractometer at the Department of Mathematics and Geosciences (University of Trieste), using MoKα radiation, monochromatized by a flat graphite crystal. Chromites from the studied meteorites are usually rather small. The longer axis in these chromite grains is up to about 120 μm, but usually below 100 μm, the other axis is between 20 and 50 μm so that in some cases the grain is nearly "two-dimensional" with a thickness of only 20 μm. Given that, for the largest grains, twenty-four equivalent reflections of (12 8 4) peak, at about 80° of 2θ, were accurately centered at both sides of 2θ, and the α_1 peak barycenter was used for cell parameter determination. For the smallest grains, forty-eight reflections of (8 4 0) and (8 4 4) peaks, at about 45-50° of 2θ, have been used. Data collection was made, according to Della Giusta *et al.* (1996), up to 50° of θ in the ω-2θ scan mode, scan width 1.8°2θ, counting time from 20 to 50 seconds depending on the peak standard deviation. Corrections for absorption and background were performed according to North *et al.* (1968). Structural refinement using the SHELX-97 program (Sheldrick, 2008) was carried out against Fo^2_{hkl} in the Fd-3m space group (with origin at -3*m*), since no evidence of different symmetry appeared. Scattering factors were taken from Prince (2004) and Tokonami (1965). Neutral scattering curves, Mg *vs*. Fe in T site and Cr *vs.* Al in M site, were assigned, with the constraints of full site occupancy and equal displacement parameters. Oxygen ionization was varied from one grain to another in order to reach the best fit between structural refinement and chemical analyses and to obtain the best value for all conventional agreement factors. Results are in Table 1.

After X-ray data collection, the same crystals used for X-ray data collection were mounted on glass slides, polished and carbon coated for electron microprobe analyses on a CAMECA-CAMEBAX microprobe at IGG-CNR, Padua, operating at 15kV and 15nA. A 20-s counting time was used for both peak and total background. Synthetic oxide standards (MgO, Fe_2O_3, MnO, ZnO, NiO, Al_2O_3, Cr_2O_3, TiO_2 and SiO_2; purity 99.99 %) and synthetic chromite and Mg-chromite (Lenaz *et al.*, 2004b) were used. Raw data were reduced by PAP-type correction software provided by CAMECA. Results are in Table 2.

Several different procedures may be adopted to determine cation distribution, and very satisfactory results have recently been obtained by combining data from single-crystal X-ray structural refinements and electron microprobe analyses. This approach simultaneously takes into account both structural and chemical data and reproduces the observed parameters by optimizing cation distributions. Differences between measured and calculated parameters are minimized by a function F(X) taking in consideration different parameters as the observed quantity and their standard deviations, cation fractions in T and M sites, unit cell and oxygen parameter, mean atomic numbers of T and M sites, atomic proportions given by microprobe analyses, and constraints imposed by crystal chemistry (total charges and occupancies of T and M sites) (see Appendix). Several minimization cycles of the equation containing these parameters were performed until convergence according to the procedures described in Carbonin *et al.* (1996) and Lavina *et al.* (2002) (Table 2 and Table 3). We should note that the program operates in order that the number of cations totals 3. As a result, the GOL samples have large F(X) values and errors because the number of cations never exceeds 2.985. A similar situation arose with the Franz1 chromite analyzed by Carbonin *et al.* (1999).

Considering the possible valence state partitioning (Papike *et al.*, 2005) we tested the effects of V_2O_5 instead of V_2O_3 without improvement. In Table 3 it is possible to observe the observed and calculated values of parameters involved in the minimization process.

4. RESULTS AND DISCUSSION

The cell edge of chromites in H6 ranges from 8.3480 (2) to 8.3501 (1) Å, while in GOL it varies from 8.3212 (3) to 8.3463 (3) Å (Table 1). The oxygen positional parameter ranges from 0.2627 (2) to 0.26298 (9) in H6 and from 0.2624 (3) and 0.26267 (9) in GOL (Table 1). These values show that there are minor differences in chromite composition and structure from the two types of chondrites. The ACAP chromite shows a cell edge equal to 8.3384 (1) Å and an oxygen positional parameter of 0.26251 (9) (Table 1).

The chemical composition of H6 and ACAP samples is rather homogeneous while GOL chromites present different compositions from one point to the other. This feature creates patch-like surfaces with local enrichment/depletion in major oxides. The analyzed chromites point to a nearly pure end-member composition with limited Al↔Cr (Al < 0.26 apfu) and $Mg\leftrightarrow Fe^{2+}$ (Mg ≤ 0.15 apfu, except for the ACAP sample) substitutions. Ferric iron is negligible in all the analyzed chromites (Table 2), a feature characteristic of other phases too, in extraterrestrial materials (Papike *et al.*, 1998). All the GOL chromites here analyzed have been assigned to the L-chondrite group (TiO_2 in the range 2.9 – 3.3 wt.%) (Table 2).

The large excess octahedral crystal field stabilization energy of Cr^{3+} (Δ $CFSE_{(oct-tet)}$ is about 160 kJ mol^{-1}; O'Neill and Navrotsky, 1984) should ensure that Cr-bearing spinels have an almost completely normal cation distribution (Urusov, 1983), meaning that about ¾ of the M site is filled by Cr. Titanium and vanadium can also be assumed to occupy this site, consequently only about 0.3 cation could be filled by other cations. Cation assignment, taking in account structural and chemical parameters, shows an ordered distribution where Al almost completely fills the balance of the M site (Table 2).

Calculation of the formulae for the chromites in the GOL samples from Kinnekulle gives a total number of cations less than 3 and a total number of electrons per formula unit significantly higher than that derived from structural refinement. In terrestrial samples this fact, coupled with a low oxygen parameter value (< 0.2620), suggested the presence of vacancies (Carbonin *et al.*, 1999; Bosi *et al.*, 2004; Lenaz *et al.*, 2014a, 2014c). The low oxygen positional parameter in terrestrial samples (in the range 0.2608-0.2620) is a product of the $3Fe^{2+} \rightarrow 2Fe^{3+}$ + vacancies transformation under oxidizing conditions. This causes the development of a magnetite component as seen from a combined X-ray single crystal diffraction and Mössbauer (MS) approach (Lenaz *et al.*, 2014a, 2014c) and exemplified by Lenaz *et al.* (2013) by comparing the results of structural refinement (SREF), microprobe analyses, point-MS and powder-MS collected on several chromite samples. They showed that in some cases there was a large discrepancy between SREF and powder-MS because commonly used powder-MS needs a lot of grains where oxidation degree could be very different among the grains, while SREF and point-MS have been performed on the same single crystal yielding a good comparison. These phenomena in the terrestrial environment are considered as the result of oxidation processes that happened after primary chromite formation at temperatures between 600-700°C. It is unlikely this oxidation processes in the present case took place on the sea floor or during diagenesis, consequently we think that this non - stoichiometry should be primary. Alwmark and Schmitz (2007) noticed in some extraterrestrial chromites from the Lockne crater in central Sweden, Zn enrichment and oxidation that they suggested to be a result of the hydrothermal system induced by the impact. In the present case there is undoubtedly a non - stoichiometry, but the absence of Zn enrichment as well as the oxygen parameters higher than 0.2624 suggest that the non-stoichiometry is not due to oxidation. Moreover, this feature has been already noticed in other extraterrestrial mineral phases (Weill *et al.*, 1971; Herd and Papike, 1998; Yurimoto *et al.*, 2001; Abreu *et al.*, 2014). Yurimoto *et al.* (2001) suggested a rapid crystallization to explain the non - stoichiometry of some spinels from a CO chondrite, while Abreu *et al.* (2014) suggested shock metamorphism for non-stoichiometry in CR chondrite grains of several unknown ferromagnesian silicates ($Fe_5MgSi_2O_{10}$, $Fe_4MgSi_3O_{11}$ and other similar compounds). We suggest that the spinels studied here present a non - stoichiometry for similar reasons.

By comparison with the structural parameters of chromites from terrestrial occurrences, in an oxygen positional parameter *vs*. cell edge diagram (Fig. 1) the extraterrestrial chromites fall in a field close to that of chromites from komatiites (Lenaz *et al.*, 2004a), kimberlites and included in diamonds (Lenaz *et al.*, 2009), and not far from that of layered intrusions (Lenaz *et al.*, 2007, 2012) and the synthetic $MgCr_2O_4$-$FeCr_2O_4$ series (Lenaz *et al.*, 2004b). When comparing the meteoritic spinels studied by us with the mantle occurrences from a structural point of view we can see that they fall in a field more or less parallel to that of the $MgCr_2O_4$-$FeCr_2O_4$ binary synthetic series (Lenaz *et al.*, 2004b). Considering that the $MgAl_2O_4$ and $FeAl_2O_4$ spinels have cell edges equal to 8.0855 and 8.1646 Å and oxygen positional parameter equal to 0.2613 and 0.2642, respectively, changes along the x-axis roughly suggest a Cr↔Al substitution (see also Lenaz and Skogby, 2013, for the hercynite-chromite synthetic series) while changes along the y-axis roughly suggest a $Mg \leftrightarrow Fe^{2+}$ (Fig. 2). Our data suggest a limited Cr↔Al substitution (Al_2O_3 is close to 6.5 wt. % for H6 and to 5.8 wt. % for GOL) and a larger $Mg \leftrightarrow Fe^{2+}$ (MgO ranges from 2 to 7 wt. %). Therefore the chromites in our meteorites (excluding the non-stoichiometric ones), those included in diamonds (Lenaz *et al*., 2009) and those from komatiites (Lenaz et al., 2004a) are on a trend (R^2=0.92). As all of these occurrences are mantle related, it is possible that this is a consequence of the degree of differentiation of the liquid from which they originated.

Hazen and Ferry (2010) defined three eras and ten stages of mineral evolution in our solar system. During the first era, the so-called Era of Planetary Accretion (>4.55 Ga), perhaps 60 different mineral species appeared as primary condensates. These planet-forming materials developed as planetesimals. As asteroids grew and began to experience modest heating by the decay of short-lived radionuclides such as ^{26}Al, the melting of ice and the subsequent alteration at low temperatures increased mineral diversity to 250 (McCoy, 2010). In fact, one of the many mechanisms that drove mineral diversification is increase in the ranges of intensive variables such as pressure, temperature and the activities of H_2O, CO_2 and O_2 (Hazen and Eldredge, 2010). Even while this aqueous alteration and thermal metamorphism were occurring in asteroids, an era of intense bombardment began. These impacts formed new minerals as chondritic asteroids were subjected to intense heat and pressure (McCoy, 2010). As heating continued, the solidus temperature of about 950°C was exceeded and melting began. The earliest partial melts formed from FeNi metal and the iron sulfide troilite, but they also incorporated minerals like chromite and phosphates (McCoy, 2010). By using the geothermometer proposed by Princivalle *et al*. (1999) an intracrystalline equilibration temperature equal or higher than about 1250°C (Table 2) has been found for H6 and ACAP chromite grains, showing that the temperature reached after heating was very high. Calculated temperatures for GOL chromites are unreliable (> 1700°C). This happened also for some terrestrial occurrences (Derbyshire *et al*. 2013) where zoning is present, so that it is possible to assume that where well-defined core-rim zoning or patches are present, as in the GOL chromites, it is not possible to use the thermometer.

5. CONCLUSIONS

Because meteoritic material on the Earth surface is rapidly altered or weathered away with the exception of chromite, similarly to what happens for terrestrial mafic – ultramafic material (Lenaz *et al*., 2009, 2014b), different methodologies have been recently developed to recognize the extraterrestrial detrital chromitic material such as relict silicate inclusions (Alwmark and Schmitz, 2009) and high-precision oxygen three-isotopes SIMS analyses (Heck *et al*., 2010). This work demonstrates that a structural study can, as well, distinguish extraterrestrial from terrestrial material and also that different chondritic (H and L) origins can be recognized. This will facilitate ongoing attempts to reconstruct the paleoflux of meteorites to Earth from resistant extraterrestrial spinel grains recovered from ancient sediments.

ACKNOWLEDGMENTS

The Italian C.N.R. financed the installation and maintenance of the microprobe laboratory in Padova. R. Carampin and L. Tauro are kindly acknowledged for technical support. This work was supported with MURST and Trieste University grants to FP (PRIN 2010-2011; 2010EARRRZ_006), FRA2009 grant to DL and an Advanced Grant from the European Research Council to BS. Sabrina Nazzareni and Roberta L. Flemming are greatly acknowledged for their valuable comments.

APPENDIX

I) Cation distribution

The cation distribution for the present samples has been achieved by using the Lavina *et al.* (2002) model. This model yields cation distribution by minimizing the weighted differences between observed crystal chemical data and data calculated from site atomic fractions. This cation distribution in the tetrahedral (T) and octahedral (M) sites must be consistent with the assumptions that:

1 – The mean atomic number (m.a.n.) corresponds to:

$$\text{m.a.n. T} = \Sigma_i\, {}^{IV}X_i N_i \qquad \text{(A1)}$$

$$\text{m.a.n. M} = \Sigma_i\, {}^{VI}X_i N_i \qquad \text{(A2)}$$

where ${}^{IV}X_i$ and ${}^{VI}X_i$ are chemical species in T and M respectively and N is their atomic number

2 – The site bond length arises from a linear contribution of each species to the tetrahedral (T-O) and octahedral (M-O) coordination distances so that:

$$\text{T-O} = \Sigma_i\, {}^{IV}X_i^{IV}D_i \qquad \text{(A3)}$$

$$\text{M-O} = \Sigma_i\, {}^{VI}X_i^{VI}D_i \qquad \text{(A4)}$$

where ${}^{IV}D_i$ and ${}^{VI}D_i$ are the cation-to-oxygen bond distances of each cation in tetrahedral and octahedral coordination, respectively.

To summarize, site atomic fractions ${}^{IV}X_i$ and ${}^{VI}X_i$ must not only satisfy the above equations, but also correspond to the atomic proportions from the chemical analyses and obey three crystal-chemical constrains: occupancies of T and M sites and formal valence. Consequently, ${}^{IV}X_i$ and ${}^{VI}X_i$ may be calculated by minimizing the following sum of residuals:

$$F(X_i) = \frac{1}{n}\sum_{j=1}^{n}\left(\frac{Oj - Cj(Xi)}{\sigma j}\right)^2 \qquad (A5)$$

Where O_j are the observed quantities with their standard deviation σ_j. O_j are the four observed crystallographic parameters (a, u and m.a.n. of T and M sites) and the chemical proportions for a total of n. $C_j(X_i)$ are the corresponding quantities calculated by means of variable cation fractions X_i.

II) Temperature calculation

Della Giusta *et al*. (1996) fitted the data of their heating experiments on spinels with the following empirical equation

$$T(°C) = C1 - C2 \cdot B + C3 \cdot B2 \qquad (A6)$$

where

$$B = Al(T)/Al_{tot} + C4 \cdot (1\text{-}Mg(T) - Al(T) + C5 \cdot (2 - (Al(M) - Mg(M)) \qquad (A7)$$

and C1 to C5 are the fitting coefficients. The second term of A7 takes into account the compositional influence of (Fe^{2+} + Fe^{3+} + Si + Mn + Zn) in the T site, and the third term (Cr + Fe^{2+} + Fe^{3+} + Ti + Ni) in the M site. Princivalle *et al*. (1999) revised the above equations obtaining the linear equation

$$T(°C) = 6640 \cdot B \qquad (A8)$$

with new coefficients C4 and C5 being 0.101 and 0.041, respectively. Obtained temperatures for the chromites studied by us are in Table 2. As happened for severely altered terrestrial chromites (Derbyshire et al., 2013), the temperatures of non-stoichiometric chromites are unreliable and, consequently, not reported.

REFERENCES

Abreu, N.M., Blond, P.A., and Rietmeijer, F.J.M. (2014) Effects of shock metamorphism on the matrix of CR chondrites: GRA 06100. *45th Lunar and Planetary Conference*, Abs. 2753.

Alwmark, C., and Schmitz, B. (2007) Extraterrestrial chromite in the resurge deposits of the early Late Ordovician Lockne crater, central Sweden. *Earth and Planetary Science Letters*, **253**, 291-303.

Alwmark, C., and Schmitz, B. (2009) Relict silicate inclusions in extraterrestrial chromite and their use in the classification of fossil chondritic material. *Geochimica et Cosmochimica Acta*, **73**, 1472-1486.

Andreozzi, G.B., and Lucchesi, S. (2002) Intersite distribution of Fe^{2+} and Mg in the spinel (sensu stricto)-hercynite series by single-crystal X-ray diffraction. *American Mineralogist*, **87**, 1113-1120.

Bosi, F., Andreozzi, G.B., Ferrini, V., and Lucchesi, S. (2004) Behavior of cation vacancy in kenotetrahedral Cr-spinels from Albanian eastern belt ophiolites. *American Mineralogist*, **89**, 1367–1373.

Bridges, J.C., Schmitz, B., Hutchison, R., Greenwood, R.C., Tassinari, M., and Franchi, I.A. (2007) Petrographic classification of Middle Ordovician fossil meteorites from Sweden. *Meteoritics & Planetary Science*, **42**, 1781-1789.

Bunch, T.E., and Keil, K. (1971) Chromite and ilmenite in non-chondritic meteorites. *American Mineralogist*, **56**, 146-157

Bunch, T.E., Keil, K., and Snetsinger, K.G. (1967) Chromite composition in relation to chemistry and texture of ordinary chondrites. *Geochimica et Cosmochimica Acta*, **31**, 1569-1582.

Bunch, T.E., Keil, K., and Olsen, E. (1970) Mineralogy and petrology of silicate inclusions in iron meteorites. *Contributions to Mineralogy and Petrology*, **25**, 297-340.

Carbonin, S., Russo, U., and Della Giusta, A. (1996) Cation distribution in some natural spinels from X-ray diffraction and Mössbauer spectroscopy. *Mineralogical Magazine*, **60**, 355-368.

Carbonin, S., Menegazzo, G., Lenaz, D., and Princivalle, F. (1999) Crystal chemistry of two detrital Cr -spinels with unusual low values of oxygen positional parameter: Oxidation mechanism and possible clues to their origin. *Neues Jahrbuch für Mineralogie Monatshefte* , 359-371.

Carraro, A. (2003) Crystal chemistry of Cr-spinels from a suite of spinel peridotite mantle xenoliths from the Predazzo Area (Dolomites, Northern Italy). *European Journal of Mineralogy*, **15**, 681-688.

Della Giusta, A., Princivalle, F., and Carbonin, S. (1986) Crystal chemistry of a suite of natural Cr-bearing spinels with 0.15 < Cr < 1.07. *Neues Jahrbuch für Mineralogie Abhlandungen*, **155**, 319-330.

Della Giusta, A., Carbonin, S., and Ottonello, G. (1996) Temperature-dependent disorder in a natural Mg - Al - Fe^{2+} - Fe^{3+} - spinel. *Mineralogical Magazine*, **60**, 603-616.

Derbyshire, E.J., O'Driscoll, B., Lenaz, D., Gertisser, R., and Kronz, A. (2013) Compositional heterogeneity in chromitite seams from the Shetland Ophiolite Complex (Scotland): implications for chromitite petrogenesis and late-stage alteration in the upper mantle portion of a supra-subduction zone ophiolite. *Lithos*, **162-163**, 279-300.

Dick, H.J.B., and Bullen T. (1984) Chromian spinel as a petrogenetic indicator in abyssal and alpine-type peridotites and spatially associated lavas. *Contributions to Mineralogy and Petrology*, **86**, 54-76.

Dodd, R.T. (1969) Metamorphism of the ordinary chondrites: A review. *Geochimica et Cosmochimica Acta*, **33**, 161-203.

Folco, L., D'Orazio, M., and Burroni, A. (2006) Frontier Mountain 93001: a coarse-grained, enstatite-augite-oligoclase-rich, igneous rock from the acapulcoite-lodranite parent asteroid. *Meteoritics & Planetary Sciences*, 1183-1198.

Ford, R.L., Benedix, G.K., McCoy, T.J., and Rushmer, T. (2008) Partial melting of H6 ordinary chondrite Kernouvé: constraints on the effects of reducing conditions on oxidized compositions. *Meteoritics & Planetary Science*, **43**, 1399-1414.

Greenwood, R.C., Franchi, I.A., Gibson, J.M., Benedix, G.K. (2012). Oxygen isotope variation in primitive achondrites: the influence of primordial, asteroidal and terrestrial processes. *Geochimica et Cosmochimica Acta* **94**, 146-163.

Greenwood, R.C., Schmitz, B., Bridges, J.C., Hutchison. R., and Franchi, I. (2007) Disruption of the L chondrite parent body: New oxygen isotope evidence from Ordovician relict chromite grains. *Earth and Planetary Science Letters*, **262**, 204-213.

Hazen, R.M., and Eldredge, N. (2010) Themes and variations in complex systems. *Elements*, **6**, 43-46.

Hazen, R.M., and Ferry, J.M. (2010) Mineral evolution: Mineralogy in the fourth dimension. *Elements*, **6**, 9-12.

Heck, P.R., Schmitz, B., Baur, H., Halliday, A.N., and Wieler, R. (2004) Fast delivery of meteorites to Earth after a major asteroid collision. *Nature*, **430**, 323-325.

Heck, P.R., Ushikubo, T., Schmitz, B., Kita, N.T., Spicuzza, M.J., and Valley, J.W. (2010) A single asteroidal source for extraterrestrial Ordovician chromite grains from Sweden and China: high-precision oxygen three-isotopes SIMS analysis. *Geochimica et Cosmochimica Acta*, **74**, 497-509.

Herd, C.D.K., and Papike, J.J. (1998) Estimates of oxygen fugacity in the basaltic shergottites from electron microprobe oxygen analyses. Workshop on the Issue “Martian meteorites: Where do we stand and where are we going?”, Houston, Texas November 2–4, 1998.

Irvine, T.N. (1967) Chromian spinel as a petrogenetic indicator. Part 2. Petrologic applications. *Canadian Journal of Earth Science*, **4**, 71-103.

Lavina, B., Salviulo, G., and Della Giusta, A. (2002) Cation distribution and structure modeling of spinel solid solutions. *Physics and Chemistry of Minerals*, **29**, 10–18.

Lenaz D., and Skogby H. (2013) Structural changes in the $FeAl_2O_4$-$FeCr_2O_4$ solid solution series and their consequences on natural Cr-bearing spinels. *Physics and Chemistry of Minerals*, **40**, 587-595.

Lenaz, D., Andreozzi, G.B., Mitra, S., Bidyananda, M., and Princivalle, F. (2004a). Crystal chemical and ^{57}Fe Mössbauer study of chromite from the Nuggihalli schist belt (India). *Mineralogy and Petrology*, **80**, 45-57.

Lenaz, D., Skogby, H., Princivalle, F., and Hålenius, U. (2004b) Structural changes and valence states in the $MgCr_2O_4$-$FeCr_2O_4$ solid solution series. *Physics and Chemistry of Minerals*, **31**, 633-642.

Lenaz, D., Braidotti, R., Princivalle, F., Garuti, G., and Zaccarini, F. (2007) Crystal chemistry and structural refinement of chromites from different chromitite layers and xenoliths of the Bushveld Complex. *European Journal of Mineralogy*, **19**, 599–609.

Lenaz, D., Logvinova, A.M., Princivalle, F., and Sobolev, N.V. (2009) Structural parameters of chromite included in diamonds and kimberlites from Siberia: A new tool for discriminating ultramafic source. *American Mineralogist*, **94**,1067-1070.

Lenaz, D., De Min, A., Garuti, G., Zaccarini, F., and Princivalle, F. (2010) Crystal chemistry of Cr-spinels from the lherzolite mantle peridotite of Ronda (Spain). *American Mineralogist*, **95**, 1323-1328.

Lenaz, D., O'Driscoll, B, and Princivalle, F. (2011) Petrogenesis of the anorthosite-chromitite association: crystal-chemical and petrological insights from the Rum Layered Suite, NW Scotland. *Contributions to Mineralogy and Petrology*, **162**,1201–1213.

Lenaz, D., Garuti, G., Zaccarini, F., Cooper, R.W., and Princivalle, F. (2012) The Stillwater Complex: The response of chromite crystal chemistry to magma injection. *Geologica Acta*, **10**, 33-41.

Lenaz, D., Skogby, H., Logvinova, A.M., Sobolev, N.V., and Princivalle, F. (2013) A micro-Mössbauer study of chromites included in diamond and other mantle-related rocks. *Physics and Chemistry of Minerals*, **40**, 671-679.

Lenaz, D., Adetunji, J., and Rollinson, H. (2014a) Determination of $Fe^{3+}/\Sigma Fe$ ratios in chrome spinels using a combined Mössbauer and single-crystal X-ray approach: application to chromitites from the mantle section of the Oman ophiolite. *Contributions to Mineralogy and Petrology*, **167**, article 958.

Lenaz, D., Youbi, N., De Min, A., Boumehdi, M.A., and Ben Abbou, M. (2014b) Low intra-crystalline closure temperatures of Cr-bearing spinels from the mantle xenoliths of the Middle Atlas Neogene-Quaternary Volcanic Field (Morocco): A mineralogical evidence of a cooler mantle beneath the West African Craton. *American Mineralogist*, **99**, 267-275.

Lenaz D., Andreozzi G.B., Bidyananda M., and Princivalle F. (2014c) Oxidation degree of chromite from Indian ophiolites: a crystal chemical and ^{57}Fe Mössbauer study. *Periodico di Mineralogia*, **83**, 241-255.

McCoy, T.J. (2010) Mineralogical evolution of meteorites. *Elements*, **6**, 19-23.

McCoy, T.J., Keil, K., Clayton, R.N., and Mayeda, T.K. (1993) Classification parameters for acapulcoites and lodranites: the cases of FRO 90011, EET 84302 and ALH A81187/84190. (Abs.) *XXIV Lunar and Planetary Science Conference*, Part 2, 945-946.

North, A.C.T., Phillips, D.C., and Scott-Mattews, F. (1968) A semi-empirical method of absorption correction. *Acta Crystallographica*, **A24**, 351-352

O'Neill, H.St.C., and Navrotsky, A. (1984) Cation distributions and thermodynamic properties of binary spinel solid solutions. *American Mineralogist*, **69**, 733–753

Palme, H., Suess, H.E., and Zeh, H.D. (1981) Abundances of the elements in the solar system. In Landolt-Börnstein, Neue Serie VI/2a, 257-272. Berlin-Heidelberg: Springer Verlag.

Papike, J.J., Ryder, G., and Shearer, C.K. (1998) Lunar samples. Papike J.J. (Ed.) Planetary materials, *Rev. in Mineralogy*, **36**, Chapter 5, 234 pp.

Papike, J.J., Karner, J.M., and Shearer, C.K. (2005) Comparative planetary mineralogy: Valence state partitioning of Cr, Fe, Ti, and V among crystallographic sites in olivine, pyroxene, and spinel from planetary basalts. *American Mineralogist*, **90**, 277-290.

Prince, E. (2004) International Tables for X-ray Crystallography. Volume C: Mathematical, physical and chemical tables. 3rd ed. Sprinter, Dordrecht, The Netherlands.

Princivalle, F., Della Giusta, A., and Carbonin, S. (1989) Comparative crystal chemistry of spinels from some suites of ultramafic rocks. *Mineralogy and Petrology*, **40**, 117-126.

Princivalle, F., Della Giusta, A., De Min, A., and Piccirillo, E.M. (1999) Crystal chemistry and significance of cation ordering in Mg–Al rich spinels from high-grade hornfels (Predazzo-Monzoni, NE Italy). *Mineralogical Magazine*, **63**, 257–262.

Princivalle, F., De Min, A., Lenaz, D., Scarbolo, M., and Zanetti, A. (2014) Ultramafic xenoliths from Damaping (Hannuoba region, NE-China): petrogenetic implications from crystal chemistry of pyroxenes, olivine and Cr-spinel and trace element content of clinopyroxene. *Lithos*, **188**, 3-14.

Rubin, A.E. (2007) Petrogenesis of acapulcoites and lodranites: a shock-melting model. *Geochimica et Cosmochimica Acta*, **71**, 2383-2401.

Schmitz, B. (2013) Extraterrestrial spinels and the astronomical perspective on Earth's geological record and evolution of life. *Chemie der Erde*, **73**, 113-135.

Schmitz, B., and Häggström, T. (2006) Extraterrestrial chromite in Middle Ordovician limestone at Kinnekulle, southern Sweden – traces of a major asteroid breakup event. *Meteoritics & Planetary Science*, **41**, 455-466.

Schmitz, B., Tassinari, M., and Peucker-Ehrenbrink, B. (2001) A rain of ordinary chondritic meteorites in the early Ordovician. *Earth and Planetary Science Letters*, **194**, 1-15.

Sheldrick, G.M. (2008) A short history of SHELX. *Acta Crystallographica*, **A64**, 112-122.

Tokonami, M. (1965) Atomic scattering factor for O^{-2}. *Acta Crystallographica*, **19**, 486.

Uchida, H., Lavina, B., Downes, R.T., and Chesley, J. (2005). Single-crystal X-ray diffraction of spinels from the San Carlos Volcanic Field, Arizona: Spinel as a geothermometer. *American Mineralogist*, **90**, 1900-1908.

Urusov, V.S. (1983) Interaction of cation on octahedral and tetrahedral sites in simple minerals. *Physics and Chemistry of Minerals*, **9**, 1–5.

Weill, D.F., Grieve, R.A., McCallum, I.S., and Bottinga, Y. (1971) Mineralogy-petrology of lunar samples. Microprobe studies of samples 12021 and 12022; viscosity of melts of selected lunar compositions. *Proceedings of the Second Lunar Science Conference*, **1**, 413-430.

Wlotzka, F. (2005) Cr spinel and chromite as petrogenetic indicators in ordinary chondrites: equilibration temperatures of petrologic types 3.7 to 6. *Meteoritics & Planetary Science*, **40**, 1673-1702.

Yurimoto, H., Rubin, A.E., Itoh, S., and Wasson, J.T. (2001) Non-stoichiometric Al-rich spinel in an ultra-refractory inclusion from CO chondrite. *Lunar and Planetary Science*, **32**, Abs. 1557.

Figure captions

Fig. 1: Oxygen positional parameter, *u* vs. cell edge, a. Red circles: H6, this study; red squares: GOL, this study; black diamond: ACAP chromite, this study; blue diamonds: chromite in kimberlites and included in diamonds (Lenaz *et al*., 2009); purple squares: chromites in komatiites (Lenaz *et al*., 2004a); yellow circles: chromites in layered intrusions (Lenaz *et al*., 2007; 2012); green circles: $MgCr_2O_4$-$FeCr_2O_4$ synthetic spinels (Lenaz *et al*., 2004b).

Fig. 2: Oxygen positional parameter, *u* vs. cell edge, a for synthetic series and the meteoritic chromites studied here. Blue squares: $MgAl_2O_4$-$FeAl_2O_4$ (Andreozzi and Lucchesi, 2002); orange diamonds: $FeAl_2O_4$-$FeCr_2O_4$ (Lenaz and Skogby, 2013); green circles: $MgCr_2O_4$-$FeCr_2O_4$ spinels (Lenaz *et al*., 2004b). The meteorite chromites of this study are represented by red circles.

Table 1: Results of crystal structure refinements of chromite

Sample	**H6-1**	**H6-2**	**H6-C**	**H6-D**	**ACAP**	**GOL-A**	**GOL-B**	**GOL-C**	**GOL-D**
a (Å)	8.3488 (1)	8.3501 (1)	8.3480 (2)	8.3485 (2)	8.3384 (1)	8.3463 (3)	8.3349 (3)	8.3347 (3)	8.3212 (3)
u	0.26286 (7)	0.26291 (7)	0.26298 (9)	0.2627 (2)	0.26251 (9)	0.26267 (9)	0.2625 (1)	0.2626 (1)	0.2624 (3)
T-O	1.994 (1)	1.995 (1)	1.995 (1)	1.992 (3)	1.987 (1)	1.990 (1)	1.985 (2)	1.989 (2)	1.980 (5)
M-O	1.9856 (5)	1.9856 (5)	1.9845 (7)	1.986 (2)	1.9854 (6)	1.9864 (7)	1.9852 (8)	1.986 (2)	1.983 (2)
m.a.n.T	23.7 (4)	24.0 (6)	24.2 (5)	24.5 (6)	21.3 (2)	23.3 (3)	22.0 (4)	24.0 (5)	22.1 (5)
m.a.n.M	22.1 (5)	22.1 (7)	22.5 (6)	22.0 (5)	22.5 (3)	22.4 (3)	21.9 (6)	22.6 (5)	22.3 (5)
U (M)	0.0038 (1)	0.0039 (1)	0.0045 (1)	0.0039 (2)	0.0045 (1)	0.0046 (1)	0.0059 (1)	0.0052 (1)	0.0059 (3)
U (T)	0.0068 (1)	0.0071 (2)	0.0075 (2)	0.0073 (3)	0.0073 (1)	0.0073 (1)	0.0081 (2)	0.0082 (2)	0.0086 (5)
U (O)	0.0059 (2)	0.0060 (3)	0.0060 (3)	0.0070 (5)	0.0063 (2)	0.0068 (2)	0.0084 (3)	0.0072 (4)	0.0085 (9)
N. refl.	155	152	122	117	177	155	127	118	85
R1	2.01	1.86	1.80	3.01	1.67	2.04	2.23	2.43	3.55
wR2	2.77	3.11	2.67	6.65	3.31	3.62	3.34	4.64	5.50
GooF	1.241	1.088	1.119	1.173	1.154	1.258	1.145	1.137	1.296
Diff. peaks	2.91; -0.99	1.63; -0.64	1.12; -0.89	2.26; -1.53	1.74; -0.84	2.33; -1.29	1.62; -0.61	2.28; -0.63	1.75; -1.21

a: cell parameter (Å); *u*: oxygen positional parameter; T-O and M-O: tetrahedral and octahedral bond lenghts (Å), respectively; m.a.n.T and M: mean atomic number; U(M), U(T), U(O): displacement parameters for M site, T site and O; N. Refl.: number of unique reflections; R1 all (%), wR2 (%), GooF as defined in Sheldrick (2008). Diff.peaks: maximum and minimum residual electron density (± e/Å^3). Space Group: Fd-3m. Origin fixed at –3m. Z=8. Reciprocal space range: $-19 \leq h \leq 19$; $0 \leq k \leq 19$; $0 \leq l \leq 19$. Estimated standard deviations in *brackets*.

Table 2. Mean chemical analyses and cation distribution of chromite

Sample	H6-1	H6-2	H6-C	H6-D	ACAP	GOL-A	GOL-B	GOL-C	GOL-D
MgO	3.35 (8)	3.3 (1)	3.2 (1)	3.0 (1)	6.9 (3)	2.3 (2)	2.9 (3)	2.0 (1)	2.67 (9)
Al_2O_3	6.5 (2)	6.4 (1)	6.46 (8)	6.7 (1)	6.1 (1)	5.9 (1)	5.8 (1)	5.8 (3)	5.78 (4)
TiO_2	2.3 (2)	2.32 (7)	2.29 (4)	2.10 (7)	1.18 (4)	3.08 (4)	3.2 (1)	2.9 (1)	3.32 (3)
V_2O_3	0.74 (6)	0.67 (5)	0.66 (3)	0.71 (6)	0.57 (3)	0.67 (1)	0.73 (5)	0.65 (5)	0.69 (1)
Cr_2O_3	56.9 (4)	56.9 (5)	57.2 (1)	56.4 (5)	61.7 (5)	57.0 (7)	57.2 (9)	57.0 (8)	56.62 (6)
MnO	0.91 (6)	0.87 (6)	0.95 (7)	0.84 (4)	1.6 (5)	0.68 (7)	0.71 (6)	0.57 (6)	0.93 (6)
FeO	28.7 (3)	29.1 (3)	29.0 (2)	29.2 (2)	21.1 (4)	29.5 (1.0)	29.0 (1.0)	28.9 (1.5)	28.6 (3)
NiO*	0.03 (3)	0.02 (3)	0.00 (0)	0.01 (1)	0.01 (1)	0.01 (1)	0.01 (1)	0.01 (1)	0.01 (1)
ZnO*	0.37 (2)	0.36 (5)	0.31 (3)	0.33 (4)	1.0 (1)	0.30 (3)	0.33 (6)		0.7 (1)
Sum	99.74	99.92	100.00	99.19	100.13	99.39	99.23	98.8	99.3
T Site									
Mg	0.152 (4)	0.107 (6)	0.110 (4)	0.101 (6)	0.32 (1)	0.105 (9)	0.16 (1)	0.07 (1)	0.089 (4)
Al	0.009 (1)	0.013 (1)	0.0090 (4)	0.020 (1)	0.017 (1)	0.027 (2)	0.0001 (1)	0.037 (5)	0.0702 (9)
Mn	0.027 (2)	0.026 (2)	0.027 (2)	0.025 (1)	0.05 (1)	0.020 (2)	0.022 (2)	0.017 (2)	0.028 (2)
Fe^{2+}	0.803 (6)	0.843 (8)	0.845 (5)	0.844 (7)	0.59 (1)	0.82 (2)	0.51 (1)	0.86 (3)	0.783 (6)
Zn	0.009 (1)	0.009 (1)	0.009 (1)	0.009 (1)	0.025 (3)	0.0079 (8)	0.010 (2)		0.018 (4)
Vac.						0.0184 (5)	0.13 (1)	0.0114 (8)	0.0104 (8)
M Site									
Mg	0.027 (2)	0.067 (5)	0.058 (3)	0.057 (4)	0.033 (4)	0.022 (4)		0.040 (7)	
Al	0.260 (5)	0.252 (5)	0.260 (2)	0.262 (4)	0.231 (4)	0.225 (6)	0.230 (6)	0.22 (1)	0.174 (1)
Ti	0.060 (3)	0.062 (2)	0.061 (1)	0.056 (2)	0.031 (1)	0.082 (2)	0.082 (3)	0.078 (3)	0.0889 (8)
V	0.021 (2)	0.019 (1)	0.0187 (8)	0.020 (2)	0.0157 (8)	0.0191 (4)	0.020 (1)	0.019 (2)	0.0197 (3)
Cr	1.593 (8)	1.588 (9)	1.592 (5)	1.584 (9)	1.68 (1)	1.61 (2)	1.52 (2)	1.61 (3)	1.609 (5)
Fe^{2+}	0.038 (1)	0.0076 (1)	0.0090 (5)	0.018 (1)	0.012 (1)	0.044 (5)		0.020 (5)	0.049 (1)
Vac.							0.006 (2)	0.0086 (7)	0.0050 (6)
T (°C)	1245	1374	1265	1512	1377				

T (°C) is the intracrystalline temperature calculated by using the thermometer of Princivalle et al. (1999). *Ni and, occasionally, Zn not present in cation distribution because of the deviation higher than 2σ. Estimated standard deviations are in brackets. High F(X) values are caused by the not-stoichiometry of the spinels with a number of cations in the range 2.980-2.984. Temperatures for non-stoichiometric chromites are unreliable and, consequently, not reported (see Appendix for details).

Table 3. Comparison of observed number of electrons, cell edge a and oxygen positional parameter u with corresponding values calculated with the MINUIT program.

Sample	**H6-1**	**H6-2**	**H6-C**	**H6-D**	**ACAP**	**GOL-A**	**GOL-B**	**GOL-C**	**GOL-D**
$e^{-}T_{obs}$	23.7 (4)	24.0 (6)	24.2 (5)	24.5 (6)	21.3 (2)	23.3 (3)	21.9 (4)	24.0 (5)	22.1 (5)
$e^{-}T_{calc}$	23.7	24.3	24.3	24.3	21.3	23.7	20.5	24.2	23.6
$e^{-}M_{obs}$	22.1 (5)	22.1 (7)	22.5 (5)	22.0 (5)	22.5 (3)	22.4 (3)	21.9 (6)	22.6 (6)	22.3 (5)
$e^{-}M_{calc}$	22.4	22.1	22.1	22.2	22.5	22.5	22.8	22.4	22.6
a_{obs}	8.3488 (1)	8.3501 (1)	8.3480 (2)	8.3485 (2)	8.3384 (1)	8.3463 (3)	8.3349 (3)	8.3439 (3)	8.3212 (3)
a_{calc}	8.3488	8.3501	8.3480	8.3485	8.3384	8.3463	8.3348	8.3439	8.3215
u_{obs}	0.26286 (7)	0.26291 (7)	0.26298 (9)	0.2627 (2)	0.26251 (9)	0.26267 (9)	0.2625 (1)	0.2626 (1)	0.2624 (2)
u_{calc}	0.26284	0.26287	0.26294	0.2627	0.26248	0.26266	0.2620	0.2626	0.2622
F(X)	0.16	0.14	0.22	0.72	0.09	0.54	4.08	0.51	8.94

F(x): minimisation factor, which takes into account the mean of square differences between calculated and observed parameters, divided by their standard deviations.

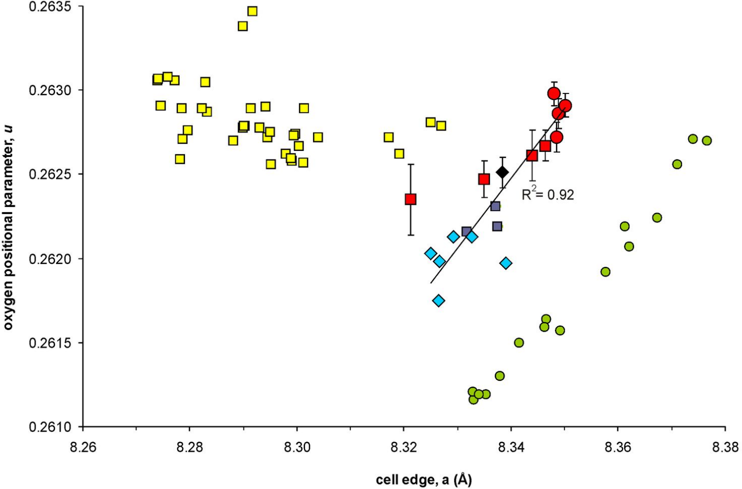
0.2635
0.2630
0.2625
0.2620
0.2615
0.2610
oxygen positional parameter, u
8.26
8.28
8.30
8.32
8.34
8.36
8.38
cell edge, a (Å)
R2= 0.92

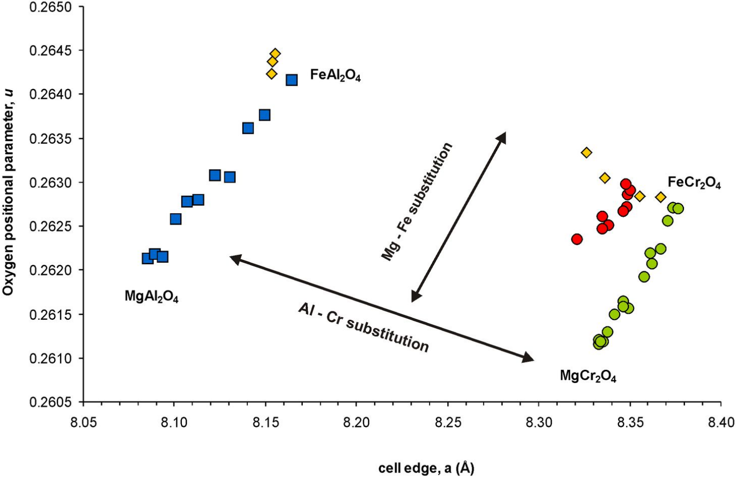
Oxygen positional parameter, *u*
0.2650
0.2645
0.2640
0.2635
0.2630
0.2625
0.2620
0.2615
0.2610
0.2605
8.05
8.10
8.15
8.20
8.25
8.30
8.35
8.40
cell edge, a (Å)
$FeAl_2O_4$
$MgAl_2O_4$
$FeCr_2O_4$
$MgCr_2O_4$
Mg - Fe substitution
Al - Cr substitution